

Multiple diffraction model for proton-proton elastic scattering and total cross section extrapolations to cosmic-ray energies

A. F. Martini and M. J. Menon
Instituto de Física ‘Gleb Wataghin’
Universidade Estadual de Campinas, Unicamp
13083-970 Campinas, SP, Brasil
(December 16, 2017)

We analyse pp elastic scattering data at the highest accelerator energy region ($10 < \sqrt{s} \leq 62.5$ GeV) through a multiple diffraction approach. The use of Martin’s formula in a model developed earlier is substituted by the introduction of a complex elementary (parton-parton) amplitude. With this the total cross section and the ρ -parameter may be simultaneously investigated and, with the exception of the diffraction minimum at some ISR energies, a satisfactory description of all experimental data is obtained. Total cross sections extrapolations to cosmic-ray energies ($\sqrt{s} > 6$ TeV) show agreement with the reanalysis of the Akeno data performed by N. N. Nikolaev and also with Gaisser, Sukhatme and Yodh results, leading to the prediction $\sigma_{tot}^{pp}(\sqrt{s} = 16 \text{ TeV}) = 147 \text{ mb}$. Physical interpretations and critical remarks concerning our parametrizations and results are also presented and discussed.

13.85.Dz, 11.80.La, 11.80.Fv

I. INTRODUCTION

Elastic proton-proton scattering is the most simple process in high-energy hadronic interactions. Despite the amount of experimental data available and model descriptions of these data, a treatment based exclusively in the field theory of strong interactions, the quantum-chromodynamics (QCD), is still missing. Beyond the intrinsic interest coming from this fact, new expectations are associated with the next proton collider, the CERN Large Hadron Collider (LHC), optimistically planned to begin experiments at 14 TeV in 2005. The situation suggests that a fundamental and difficult task for present and future developments, is to find connections between model descriptions and reliable calculational schemes in QCD. Since elastic scattering incorporates soft processes one expects that nonperturbative formalisms will play a fundamental role.

Based on the above considerations we have investigated elastic proton-proton scattering through phenomenological approaches and, simultaneously, looking for connections with nonperturbative QCD treatments. With this strategy, we improved some aspects of a multiple diffraction model developed earlier. The main points concern the use of a complex elementary (parton-parton) amplitude instead of Martin’s real-part formula and the selection of more suitable parametrizations for the free parameters. With this, we achieved a good (but limited)

description of the main physical observables in the accelerator energy domain. Based on these satisfactory results we extrapolate our parametrizations to cosmic-ray energies in order to investigate total cross sections.

In this report we present in some detail all the underlying aspects of the work, related to both the technical matters and to the general ideas and physical interpretations.

The material is organized as follows. In Sec. II we briefly recall the experimental status (accelerator and cosmic-ray data) on pp scattering and outline a survey of some theoretical results that show the present relevance of the multiple diffraction formalism. In Sec. III we describe the model, the improvements introduced, the predictions for the physical observables in the accelerator energy region and the extrapolations to cosmic-ray energies. Discussions, physical interpretations and critical remarks concerning the main results are the content of Sec. IV.

II. EXPERIMENTAL AND THEORETICAL CONTEXTS

Elastic pp scattering is essentially characterized by three physical observables: differential cross section, total cross section and the ρ -parameter (ratio of the forward real to imaginary part of the scattering amplitude). From these, others quantities may be derived such as the slope parameter and integrated elastic and inelastic cross sections [1].

Experimental data on these observables obtained and compiled nearly fifteen years ago, still remain the only source of information at high-energies extending up to $\sqrt{s} = 62.5$ GeV, the CERN Intersecting Storage Ring (ISR) energy region [2,3]. Experimental information on pp total cross sections in the range of energy $\sqrt{s} : 6 - 40$ TeV exists from cosmic-ray data on Extensive Air Showers [4–6]. However, since the proton cross section is extracted from the proton-air cross section through phenomenological models [5] the results are model dependent. Also, the analysis performed by the Akeno Collaboration [4] was recently criticized by N.N. Nikolaev who claimed that the Akeno results have been underestimated by about 30 mb [6] and this is in agreement with the results early obtained by Gaisser, Sukhatme and Yodh [5]. This is a central point in our work and we will discuss

this discrepancy in Secs. III and IV. Anyway, before the CERN's LHC proton-proton collider, cosmic-ray results remain the only source of information on pp interactions at the highest energies.

From the theoretical point of view it is well known that a pure QCD description of the elastic hadron scattering has not yet been obtained. Perturbative QCD cannot be extended to the soft region and pure nonperturbative QCD is not able to predict scattering states. Although the bulk of experimental data has been successfully described by different models in different contexts [7], a widely established and accepted approach is still missing. The same can be said of a pure QCD understanding of the subject.

As stated before, we are interested in the interface phenomenology/ nonperturbative QCD. For this we will limit this introductory discussion to some ideas directly related to this subject.

Despite the above difficulties, there has been in recent years important progresses in the framework of nonperturbative QCD, concerning soft processes. Looking for a microscopic approach able to explain phenomenological results, Landshoff and Nachtmann associated the Pomeron to the exchange of two abelian gluons with modified propagators [8]. Following this analysis, Nachtmann extended the approach to the case of non-abelian gluons in a functional representation of scattering matrix elements and eikonal approximation [9]. With this, the quark-quark amplitudes are associated with a gluonic correlation function. However, since physical observables are connected with hadron-hadron amplitudes, a central problem concerns the construction of these amplitudes from the elementary ones.

One way to treat this problem is based on the stochastic vacuum model [10]. The hadronic amplitude is constructed through scattering amplitudes for Wilson loops in Minkowski space-time (loop-loop scattering), leading to gauge invariant amplitudes [11]. With this nonperturbative framework general characteristics concerning total cross sections and slope parameters in high-energy hadron-hadron scattering may be described [11].

Another way to construct the hadronic amplitude from the elementary one is by means of Glauber's multiple diffraction theory [12] and this is the point we are interested in. The approach is based on the impact parameter and eikonal formalisms as follows: Assuming azimuthal symmetry in the collision of two hadrons A and B, the impact parameter formalism connects the eikonal χ and the elastic hadronic scattering amplitude by [12]

$$F(q, s) = i \int_0^\infty b db [1 - e^{i\chi(b, s)}] J_0(qb) \equiv i < 1 - e^{i\chi(b, s)} >, \quad (1)$$

where $q^2 = -t$ is the four-momentum transfer squared, b the impact parameter, J_0 the zero-order Bessel function and the angular brackets denotes the symmetrical two-dimensional Fourier transform. In the first order Glauber

multiple diffraction theory the eikonal is expressed as the Fourier transform of the products of the hadronic form factors, G_A and G_B , by the averaged elementary (parton-parton) amplitude f , [13], namely:

$$\chi(b, s) = \langle G_A G_B f \rangle. \quad (2)$$

This approximation means that at any time one constituent of a hadron interacts with only one constituent of the other hadron. This corresponds to the generalized form of the Chou-Yang model [14], once a well-defined Fourier transform for the elementary amplitude is assumed [15].

The importance of this phenomenological framework in the search for connections between experimental data and calculational schemes in nonperturbative QCD has been recently expressed in the work by Grandel and Weise [16]. Making use of the Dosch and Krämer ansatz for the gluonic correlation function [11] the authors calculated the elementary (parton-parton) amplitude $f(q)$ in the high-energy approximation. Then, introducing a monopole parametrization for the unknown hadronic form factors in (2) the hadronic amplitude (1) could be calculated, leading to the differential cross section. With this, the authors obtained a satisfactory description of the differential cross section data for pp and $\bar{p}p$ elastic scattering at ISR and CERN Super Proton Synchrotron (Sp \bar{p} S) energies, in the region of small transfer momentum ($q^2 \lesssim 2.0 \text{ GeV}^2$) [16].

Despite all these developments we see that the connections between nonperturbative QCD approaches and the bulk of physical observables still depends strongly on phenomenological models and ad hoc parametrizations. In this sense we understand that the role of a constant feedback on phenomenological information is crucial for present and future developments.

In particular we see that the multiple diffraction formalism may be a powerful tool in the test of suitable parametrizations. Simultaneously it may contribute with the search of reliable calculational schemes at different levels of the theory (e.g. the stochastic vacuum model). We stress also the importance of the energy dependences which may be extracted from parametrizations for the form factors and elementary amplitudes. Since the theoretical approaches (nonperturbative) mentioned above make use of asymptotic energy limits, the full increase of the total cross section, the shrinkage of the diffraction peak, the energy dependence of the ρ -parameter and even possible residual differences between pp and $\bar{p}p$ scattering at the highest energies have not yet been explained.

Based on all these considerations, in the next sections we will investigate elastic pp scattering in the context of a multiple diffraction model.

III. MULTIPLE DIFFRACTION MODEL

A. Previous approach and Martin's formula

From a phenomenological point of view, multiple diffraction models are currently identified by each particular choice of parametrizations for the form factors, G_A, G_B and elementary amplitude, f in Eq. (2) [15]. With this, the hadronic amplitude (1) may be investigated and then, in principle, the physical observables referred to in the beginning of Sec. II

$$\frac{d\sigma}{dq^2} = \pi |F(q, s)|^2, \quad (3)$$

$$\sigma_{tot}(s) = 4\pi \text{Im}\{F(q=0, s)\}, \quad (4)$$

$$\rho(s) = \frac{\text{Re}\{F(q=0, s)\}}{\text{Im}\{F(q=0, s)\}}. \quad (5)$$

In a previous approach, elastic pp and $\bar{p}p$ scattering were investigated in a multiple diffraction model through the following parametrizations for the form factors and elementary amplitude [17,18]

$$G = \left(1 + \frac{q^2}{\alpha^2}\right)^{-1} \left(1 + \frac{q^2}{\beta^2}\right)^{-1} \quad (6)$$

$$f = iC \frac{1 - \frac{q^2}{a^2}}{1 + \frac{q^4}{a^4}} \quad (7)$$

where α^2, β^2, a^2 and C are free parameters. We introduced here a small change in the previous notation of the elementary amplitude which will be suitable in what follows.

The justifications for the above parametrizations were extensively discussed and explained in [18] and [19] and will not be reproduced here. We only recall that Eq. (7) is in agreement with the results from model-independent analysis for the dynamical part of the eikonal as obtained by Buenerd, Furget, and Valin [20] and Carvalho and Menon [21]. Discussion on this subject may be found in [15] and [22].

With the parametrizations (6) and (7) the eikonal in (2) is purely imaginary and so the hadronic amplitude (1). In the previous approach the real part of this amplitude was estimated through Martin's formula [23]

$$\text{Re}F(q, s) = \frac{d}{dq^2} [\rho q^2 \text{Im}F(q, s)], \quad (8)$$

using the experimental ρ value at each energy. With this approach a satisfactory description of experimental data on differential and integrated cross sections was obtained [17,19,24].

However, a crucial point concerns the use of the above formula and this deserves some discussion. First, as derived by Martin the formula holds only for values of

the momentum transfer infinitesimally small and at the asymptotically high-energy regime [23]. The formula may also be derived through the geometrical scaling hypothesis [25] and in this case its applicability should be limited to the ISR energy region. Corrections to Martin's formula were introduced by Henzi and Valin [26] and numerical analysis from fits of experimental data by Kundrát and Lokajicěk puts serious limits in its applicability concerning momentum transfer [27]. This result however has been recently criticized by Kawasaki, Maehara and Yonezawa who present results favouring the applicability of the formula in the whole region of the momentum transfer with the data available [28].

Despite this controversial aspect, a serious problem with the use of Martin's prescription is that $\rho(s)$ is an input parameter at each energy and so cannot be investigated. This led us to try a different procedure in the determination of the real part of the hadronic amplitude and in the next section we introduce a possible solution for the problem.

B. Complex elementary amplitude

In the context of the multiple diffraction formalism, Eqs. (1) and (2), associated with a complex hadronic amplitude, F_{AB} , one should expect a complex elementary (parton-parton) amplitude

$$f(q, s) = \text{Re}f(q, s) + i\text{Im}f(q, s).$$

In this sense, the approach discussed in the last section corresponds to the assumption of $\text{Re}f(q, s) = 0$ and

$$\text{Im}f(q, s) = C \frac{1 - \frac{q^2}{a^2}}{1 + \frac{q^4}{a^4}}. \quad (9)$$

Lacking both theoretical and experimental information about the elementary phase we will assume, as a first approximation, a proportionality relation between real and imaginary parts at each energy [29]

$$\text{Re}f(q, s) = \lambda(s)\text{Im}f(q, s), \quad (10)$$

where $\lambda(s)$ is a free parameter. With this assumption the eikonal in (2) may be expressed by

$$\chi(b, s) = (\lambda + i)\Omega(b, s) \quad (11)$$

where, for the proton-proton case,

$$\Omega(b, s) = \langle G^2 \text{Im}f(q, s) \rangle, \quad (12)$$

with G given by (6) and $\text{Im}f(q, s)$ by (9). With this, the real and imaginary parts of the hadronic amplitude read

$$\text{Re}\{F(q, s)\} = \langle e^{-\Omega(b, s)} \sin(\lambda\Omega(b, s)) \rangle, \quad (13)$$

$$\text{Im}\{F(q, s)\} = \langle 1 - e^{-\Omega(b, s)} \cos(\lambda\Omega(b, s)) \rangle. \quad (14)$$

Substituting parametrizations (6) and (9) for G and Imf in (12), the “opacity” $\Omega(b, s)$ is analytically evaluated. Then, Eqs. (13) and (14) lead to the differential cross section (3).

As a first test of the ansatz (10) we calculate the imaginary part of the hadronic amplitude, using yet the parametrizations from the previous approach [17,18]; then the real part was evaluated through both, Martin’s prescription (8) and the ansatz (10). For pp elastic scattering at $\sqrt{s} = 52.8$ GeV (largest interval in momentum transfer with data available, [3]) the differential cross section is well described for $\lambda = 0.055$ and we display both results in Fig. 1.

We see that the predictions for the real part are similar in both cases: they present two zeros (change of sign) and its contributions to the differential cross sections are important only in the dip region.

Since the imaginary part of the amplitude presents a zero and the real part of the Martin formula is obtained by the derivative (8), the contribution of this part is out of phase and then the differential cross sections does not vanish in the dip region [23]. With the assumption (10) for the elementary amplitude the same effect is obtained in the hadronic amplitude due to sin and cos terms in (13), (14), and the result is in qualitative agreement with the predictions of zeros (change of sign) from dispersion relation [30].

Based on this satisfactory result with the complex elementary amplitude, we investigated the simultaneous descriptions of all physical observables referred before, Eqs. (3), (4) and (5). To our knowledge this has never been achieved through geometrical or multiple diffraction models and we will return to this point later.

Trying global descriptions for pp elastic scattering, besides the use of the complex elementary amplitude, we re-analysed the fits and parametrizations, improving some aspects of the previous approach. We discuss in detail the central points in what follows.

C. Fits of experimental data

As explained in the last two sections, our approach has only five free parameters: two associated with the form factor, α^2 and β^2 , and three with the elementary amplitude, C , a^2 and λ .

We analysed 7 sets of pp experimental data above 10 GeV (Table I) and the fits were performed only of the differential cross section data [3,31] and ρ parameter data [2,32] at each energy. The fit procedure consists of two steps:

1. Taking $\lambda = 0$ in Eq. (11) the hadronic amplitude, Eqs. (13) and (14), is purely imaginary. For this case we determined the values of the parameters C , α^2 , β^2 and a^2 that reproduce the differential cross section data at each energy so as to present the zero at the dip position.

2. With the values of the above four parameters as input we then calculated the value of λ that reproduces the experimental ρ value at each energy.

Step 1 comes essentially from the previous approach and has been discussed and explained in detail in [19].

With the above procedure a satisfactory description of ρ and $d\sigma/dq^2$ experimental data was obtained with two constant free parameters

$$a^2 = 8.20 \text{ GeV}^2, \quad \beta^2 = 1.80 \text{ GeV}^2, \quad (15)$$

and only three parameters depending on the energy: $C(s)$, $\alpha^2(s)$ and $\lambda(s)$. The values are shown in Table I for each set analysed.

In order to obtain a formalism able to make predictions to other energies we then proceed to investigate parametrizations for the data displayed in Table I.

D. Parametrizations as a function of the energy

The choice of suitable and consistent parametrizations is a crucial point, mainly concerning extrapolations. We will discuss this aspect in detail in what follows and also in Sec. IV. We first analyze the dependences of C and α^{-2} , which determines the imaginary part of the hadronic amplitude (and so the total cross section) and after the dependence of λ (associated only with the real part of the amplitude).

The values of C and α^{-2} from Table I are displayed in Fig. 2 and we see that both increase with the energy, presenting positive curvatures.

Experimentally, total cross sections grow like $[\ln s]^n$, $n = 1$ or 2 , at and above ISR and there is indication of “qualitative” saturation of the Martin-Froissart bound, $n = 2.2 \pm 0.3$ [33,7]. Also, from gauge field theory, lowest order cross sections for particle production (unitarity) present $\ln s$ terms [34,35]. Based on these facts and from the behaviour shown in Fig. 2, we introduced fits through polynomials

$$\sum_{n=0}^N a_n \left[\ln \frac{s}{s_0} \right]^n,$$

which is different from our early parametrizations [17–19]. Both sets of points are statistically consistent with polynomials of second degree [36] and through linear regression we obtained [37]

$$C(s) = 14.3 - 1.65[\ln(s)] + 0.159[\ln(s)]^2, \quad (\text{GeV}^{-2}) \quad (16)$$

$$\frac{1}{\alpha^2} = 2.57 - 0.217[\ln(s)] + 0.0243[\ln(s)]^2, \quad (\text{GeV}^{-2}) \quad (17)$$

and we took $s_0 = 1 \text{ GeV}^2$. In Fig. 2 we show the above parametrizations together with the fit values from Table I. Physical interpretations and critical remarks concerning parametrizations (16) and (17) will be presented in Sec. IV B.

In the case of parameter λ the choice of a suitable parametrization demands further discussions. Empirical analysis of the influence of λ in the hadronic amplitude showed that its behaviour is similar to that of the ρ parameter. That is, if λ increases (decreases) also ρ increases (decreases) and $\lambda = 0$ at the same energy value where $\rho = 0$. We will return to this point in Sec. IV C. Since there is no experimental information on $\rho(s)$ above 62.5 GeV we have, in principle, serious limitations in the choice of parametrizations. That is, in order to make extrapolations to high energies in our strictly phenomenological approach, we should infer the ρ behaviour or investigate limiting cases. With this last possibility in mind, we recall the general belief that, above $\sqrt{s} \sim 100$ GeV, $\rho(s)$ has a maximum and then goes asymptotically to zero through positive values [7]. However, how fast this happens depends on model assumptions. In order to test these possibilities we considered two different approaches to zero, which could be understood as some kind of limiting cases, that is, slow and fast convergences. The point as we shall show is to investigate the influence of these assumptions in the description of the experimental data.

In Fig. 3 we display the values of λ from Table I. Based on this behaviour and on the above considerations we introduce the following general parametrization:

$$\lambda(s) = \frac{A_1 \ln(s/s_0)}{1 + A_2 [\ln(s/s_0)] + A_3 [\ln(s/s_0)]^2}. \quad (18)$$

In this formula s_0 controls the point where $\lambda(s)$ (and $\rho(s)$) reaches zero and A_i , $i = 1, 2, 3$ the maximum and asymptotic behaviour. As the two limiting cases we took:

$$\begin{aligned} \text{Case 1 : } A_1 &= 6.95 \times 10^{-2}, \quad A_2 = 0.118, \\ A_3 &= 1.50 \times 10^{-2} \end{aligned} \quad (19)$$

$$\begin{aligned} \text{Case 2 : } A_1 &= 9.08 \times 10^{-2}, \quad A_2 = 0.318, \\ A_3 &= 1.70 \times 10^{-10} \end{aligned} \quad (20)$$

and $s_0 = 400 \text{ GeV}^2$ in both cases. Figure 3 shows these parametrizations up to $\sqrt{s} = 10^5 \text{ GeV}$.

With the parametrizations for $C(s)$, $\alpha^{-2}(s)$ and $\lambda(s)$, Eqs. (16), (17) and (18), respectively (cases 1 and 2), and result (15) for the remaining parameters β^2 and a^2 , all free parameters are completely determined. Through the formalism described in Secs. III A and III B, Eqs. (6), (9) and (12) to (14), the three physical observables (3), (4) and (5) may be predicted.

E. Model predictions and experimental data

As explained in Sec. III C our fits were performed only on differential cross section and ρ parameter data in the interval $\sqrt{s} = 13.8 - 62.5 \text{ GeV}$. In this session we first check the predictions in the interval $\sqrt{s} = 10 - 100 \text{ GeV}$ (accelerator energy region) and then display the extrapolations up to 10^5 GeV (cosmic-ray energies and future accelerators).

- Accelerator energy region

Figures 4 and 5 show the model predictions (cases 1 and 2) for the pp differential cross section, ρ parameter and total cross sections, together with the experimental data available. We observe that in this interval, cases 1 and 2 are distinguishable only for $\rho(s)$ and $\sigma_{tot}^{pp}(s)$ and below $\sqrt{s} \sim 15 \text{ GeV}$. With the exception of the diffraction minimum (dip) at the highest ISR energies, the agreement with the experimental data is quite good. In Sec. IV C we will return to this overestimation of the differential cross section in the dip region.

- Extrapolations to higher energies

Assuming that our parametrizations hold at higher energies we calculate the predictions for $\rho(s)$, $\sigma_{tot}^{pp}(s)$ up to $\sqrt{s} = 10^2 \text{ TeV}$ (cosmic-ray region) and for the differential cross sections at 10, 15 and 20 TeV (future LHC).

We show in Fig. 6 the predictions for $\rho(s)$ in cases 1 and 2 (Fig. 5) and the experimental data available. We understand that case 1 should be the most reliable from a conservative point of view. The similarities between $\rho(s)$ and $\lambda(s)$ (Fig. 3) will be discussed in Sec. IV C.

The predictions for the total cross section are shown in Fig. 7, together with accelerator data (Fig. 5) and results from cosmic-ray experiments which, due to the existing discrepancies, we briefly review in what follows.

The information available on proton-proton total cross section, σ_{tot}^{pp} , from cosmic-ray air showers are obtained through the p-air inelastic cross section, σ_{p-air}^{inel} . However, either the determination of the σ_{p-air}^{inel} or the relation between σ_{p-air}^{inel} and σ_{tot}^{pp} are model dependent [5]. In the detailed analysis of data from Fly's eyes experiment, Gaisser, Sukhatme and Yodh (GSY hereafter), estimated the limit

$$\sigma_{tot}^{pp} \geq 130 \text{ mb at } \sqrt{s} \sim 30 \text{ TeV}.$$

Making use of the Chou-Yang relation between σ_{tot}^{pp} and the slope parameter, they calculated [5]

$$\sigma_{tot}^{pp} = 175_{-27}^{+40} \text{ mb at } \sqrt{s} = 40 \text{ TeV}.$$

More recently, based on analysis of the extensive air shower, the Akeno Collaboration presented results in the interval $\sqrt{s} : 6 - 25 \text{ TeV}$. In particular they found [4]

$$\sigma_{tot}^{pp} = 133 \pm 10 \text{ mb at } \sqrt{s} = 40 \text{ TeV},$$

which is incompatible with the GSY result. However, Nikolaev showed that σ_{p-air}^{inel} inferred by the Akeno group should be identified with an absorption cross section and that this originates an increase of ~ 30 mb in the Akeno results for σ_{tot}^{pp} . From the Nikolaev analysis [6],

$$\sigma_{tot}^{pp} = 160 - 170 \text{ mb at } \sqrt{s} = 40 \text{ TeV},$$

which is in agreement with the GSY calculation.

Although the Akeno results are usually referred to in the literature, the analysis either by Nikolaev or by GSY seems correct and both are incompatible with Akeno.

All these informations are displayed in Fig. 7, together with accelerator data and our predictions in cases 1 and 2. We see that the model predictions are in complete agreement with Nikolaev and GSY results and this implies in a faster increase of the total cross section than usually believed. In particular we predict

$$\sigma_{tot}^{pp} = 147 \text{ mb at } \sqrt{s} = 16 \text{ TeV},$$

and

$$\sigma_{tot}^{pp} = 176 \text{ mb at } \sqrt{s} = 40 \text{ TeV}.$$

Further discussion on the subject will be presented in Sec. IV A.

Concerning the differential cross section, we calculate the predictions in the region to be reached by the CERN's LHC, which are displayed in Fig. 8. The results present no dip but a shoulder at $|t| \sim 0.5 \text{ GeV}^2$ and at $|t| > 4 \text{ GeV}^2$ the curves decrease smoothly with no other structures.

IV. DISCUSSION

The model described presents three parameters that depend on energy: α^2 , C and λ . In this last section we discuss some critical points and physical interpretation concerning the parametrizations and predictions.

A. High-energy extrapolations and total cross sections

Our parametrizations (16) and (17) for $C(s)$ and $\alpha^{-2}(s)$, respectively, were based on experimental information only in the interval $13.8 \leq \sqrt{s} \leq 62.5 \text{ GeV}$ and in both cases the points indicate an increase with the energy (Table I, Fig. 2). A crucial question concerns this limited region since different explicit parametrizations, statistically consistent with the set of points, may differ arbitrarily when extrapolated to higher energies.

However, constraints on the choice of parametrizations may be found through physical information available and this played an important role in our approach. As mentioned in Sec. III D, our strategy was based on the general assumption of the expected $\ln s$ - behaviour of soft

processes and on the reasonable hypothesis of polynomial functions on $\ln s$. With these constraints, we have a linear system in the free parameters of the polynomials (with the exception of the assumed value $s_0 = 1 \text{ GeV}$) and the statistical solution is unique [36], leading to the forms (16) and (17) which describe the points quite well.

On extrapolating the predictions for the total cross section to cosmic-ray energies, our results agree very well with both analyses by Nikolaev [6] and by Gaisser, Sukhatme and Yodh [5] (Fig. 7). Since the approaches by these authors are totally independent of the considerations and assumptions we have made, and, as far as we know, there is no criticism concerning their results, the agreement shown in Fig. 7 suggests a real increase of the pp total cross section faster than generally expected. In particular we predict

$$\sigma_{tot}^{pp} = 91.6 \text{ mb at } \sqrt{s} = 1.8 \text{ TeV},$$

which is higher than even the CDF result for $\bar{p}p$, $\sigma_{tot}^{\bar{p}p} = 80.03 \pm 2.24 \text{ mb}$ [39]. This seems to favour the ‘‘Odderon hypothesis’’ [40], a problem which still ‘‘remains entirely open both from the theoretical as well as from the experimental point of view’’ [41].

B. Blackening and expansion

The parameter α^2 coming from the hadronic form factor (6) is associated with the radius defined by

$$R^2(s) = -6 \frac{dG(q, s)}{dq^2} \Big|_{q^2=0}$$

and from (6)

$$R(s) = (0.483) \left[\frac{1}{\alpha^2(s)} + \frac{1}{\beta^2} \right]^{\frac{1}{2}} (fm). \quad (21)$$

Through parametrization (17) for α^{-2} and $\beta^2 = 1.80 \text{ GeV}^2$, Eq. (15), the radius increases with the energy as shown in Fig. 9. We can then interpret the parameter α^2 as associated with the well known ‘‘expansion effect’’ [35].

The parameter C corresponds to the ‘‘absorption constant’’ in the Chou-Yang picture [14,42] and is associated with the number of constituent partons in the context of the Glauber approach [12,13]. It then controls the ‘‘blackening effect’’ coming from the absorption. Our results, as in the previous approach [17,19], mean that hadrons become blacker and simultaneously larger as the energy increases, in agreement with the ‘‘BEL behaviour’’ (Black, Edgie and Large) found by Henzi and Valin [43].

These effects may be investigated through the behaviour of the Inelastic Overlap Function, $G_{in}(b, s)$, which is calculated from the unitarity condition in the impact parameter space [44]

$$2Re\Gamma(b, s) = |\Gamma(b, s)|^2 + G_{in}(b, s), \quad (22)$$

where $\Gamma(b, s)$ is the Profile Function, the Fourier transform of the hadronic amplitude (1):

$$\Gamma(b, s) = 1 - e^{i\chi(b, s)}. \quad (23)$$

In Fig. 10 we show $G_{in}(b, s)$ as function of the energy and for some fixed values of the impact parameter b . In the region 10 to 100 GeV (part (a)) we observe the simultaneous increase of G_{in} at all values of the impact parameter. In part (b) we show the central ($b = 0$) and peripheral ($b = 1fm$) regions extrapolated to $\sqrt{s} = 10^5$ GeV. We observe that in the central region the curvature becomes negative above $\sqrt{s} = 100 \sim 200$ GeV and in the peripheral region, above $\sqrt{s} \sim 10^3$ GeV. The black disc limit ($G_{in} = 1$) however seems very far to be reached, i.e., much higher than 10^5 GeV.

Since $C(s)$ and $\alpha^2(s)$ control the blackening and expansion effects, respectively, the dimensionless quantity $C\alpha^2$ gives information on the influence of each effect as function of the energy. Figure 11 shows the predictions obtained by means of parametrizations (16) and (17) up to 10^5 GeV, together with the values from fit (Table I). We observe a minimum at $\sqrt{s} \sim 30$ GeV, a change of sign in the curvature (becomes negative) above $\sqrt{s} \simeq 10^3$ GeV and the asymptotic limit value ~ 6.5 (from the parametrizations).

C. Forward real-to-imaginary ratios of the partonic and hadronic amplitudes

An essential characteristic of the Glauber multiple diffraction formalism is to connect elastic scattering cross sections for composite particles (originally nuclei and after nucleons) with the scattering amplitudes of their individual components (originally nucleons and after partons, respectively) [12,13,45]. In this context, the assumption (10) of proportionality between real and imaginary parts of the elementary (parton-parton) amplitude means that, in particular,

$$\lambda(s) = \frac{Re f(q=0, s)}{Im f(q=0, s)},$$

i.e., at the partonic level $\lambda(s)$ plays the same role as $\rho(s)$ at the hadronic level, Eq. (5). The similarities referred to in Sec. IIID between $\lambda(s)$ and $\rho(s)$ may be seen by comparisons of Figs. 3 and 6 (cases 1 and 2).

The hypothesis that λ does not depend on the momentum transfer is a very simple one and has been used here only as an ansatz. Despite this, from Fig. 1 the resulting contribution of the real part of the hadronic amplitude to the differential cross section is in qualitative agreement with the results obtained through Martin's prescription.

On the other hand, in the context of our approach, the limitations of this simple ansatz appear when we try simultaneous descriptions of cross sections (differential and total) and the ρ parameter. As we show in Fig. 4,

the predictions overestimate the differential cross section in the dip region at the highest ISR energies, leading to a limited description of the set of physical observables. With the exception of this point, all the predictions are in agreement with the experimental data (Figs. 4 and 5). Since the total cross section is calculated from the imaginary part of the hadronic amplitude our novel results at cosmic-ray energies are independent of the effect in the dip region.

We observe that the ansatz (10) may be formally equivalent to some other geometrical and multiple diffraction models characterized by complex eikonals [20,45–47]. The novel point here was to treat this hypothesis explicitly and investigate its consequence in the context of the Glauber approach, as, for example, the strong correlation between $\rho(s)$ and $\lambda(s)$ seen in Figs. 3 and 6.

To our knowledge, simultaneous and complete descriptions of cross sections (differential and total) and the ρ parameter, still remain an open problem in geometrical and multiple diffraction models. For this reason, we hope, our results may bring insights for further and deeper developments.

ACKNOWLEDGMENTS

We are thankful to Capes and CNPq for financial support.

-
- [1] M.M. Block and R.N. Cahn, *Rev. Mod. Phys.* **57**, 563 (1985).
 - [2] Experimental data on ρ and total cross sections between 23.5 and 62.5 GeV: U. Amaldi and K.R. Schubert, *Nucl. Phys.* **B166**, 301 (1980).
 - [3] Differential cross section data between 23.5 and 62.5 GeV: K.R. Schubert, "Tables on nucleon-nucleon scattering", in *Landolt-Börnstein, Numerical Data and Functional Relationships in Science and Technology, New Series, Vol. I/9a* (1979).
 - [4] M. Honda *et al.*, *Phys. Rev. Lett.* **70**, 525 (1993).
 - [5] T.K. Gaisser, U.P. Sukhatme, and G.B. Yodh, *Phys. Rev.* **D36**, 1350 (1987).
 - [6] N.N. Nikolaev, *Phys. Rev.* **D48**, R1904 (1993).
 - [7] G. Matthiae, *Rep. Prog. Phys.* **57**, 743 (1994).
 - [8] P. Landshoff and O. Nachtmann, *Z. Phys.* **C35**, 405 (1987).
 - [9] O. Nachtmann, *Ann. Phys. (N.Y.)* **209**, 436 (1991).
 - [10] H.G. Dosch, *Phys. Lett.* **B190**, 177 (1987); H.G. Dosch and Yu.A. Simonov, *Phys. Lett.* **B205**, 339 (1988).
 - [11] H.G. Dosch, E. Ferreira, and A. Krämer, *Phys. Lett.* **B289**, 153 (1992); *Phys. Lett.* **B318**, 197 (1993); *Phys. Rev.* **D50**, 1992 (1994).
 - [12] R.J. Glauber, in *Lectures in Theoretical Physics*, edited by W.E. Britten *et al.* (Interscience, New York, 1959),

- Vol. I, p. 315; *High Energy Physics and Hadron Structure*, edited by S. Devons *et al.* (Plenum, New York, 1970), p. 207.
- [13] W. Czyż and L. C. Maximon, *Ann. Phys. (N.Y.)* **52**, 59 (1969); V. Franco and G. K. Varma, *Phys. Rev. C* **18**, 349 (1978).
- [14] T.T. Chou and C.N. Yang, *Phys. Rev.* **175**, 1832 (1968).
- [15] M.J. Menon, *Phys. Rev. D* **48**, 2007 (1993).
- [16] U. Grandel and W. Weise, *Phys. Lett.* **B356**, 567 (1995).
- [17] M.J. Menon and B.M. Pimentel, *Hadronic J.* **16**, 137 (1993).
- [18] M.J. Menon, *Nucl. Phys. B (Proc. Suppl.)* **25**, 94 (1992).
- [19] M.J. Menon, *Canadian J. Phys.* **74**, 594 (1996).
- [20] C. Furget, M. Buenerd, and P. Valin, *Z. Phys C* **47**, 377 (1990).
- [21] P.A.S. Carvalho and M.J. Menon, in *1996 XVII Brazilian National Meeting on Particles and Fields*, Serra Negra, SP, 1996 (to be published); Report No. IFGW ABSTRACTA C ,1996.
- [22] A.F. Martini, M.J. Menon, and D.S. Thober, *Phys. Rev. D* **54**, 2385 (1996).
- [23] A. Martin, *Lett. Nuovo Cimento* **7**, 811 (1973).
- [24] M.J. Menon, *Hadronic J.* **16**, 47 (1993).
- [25] J. Dias de Deus, *Nucl. Phys.* **B59**, 231 (1973); *Il Nuovo Cimento* **28**, 114 (1975); A.J. Buras and J. Dias de Deus, *Nucl. Phys.* **B71**, 481 (1974).
- [26] R. Henzi and P. Valin, *Phys. Lett.* **B149**, 239 (1984).
- [27] V. Kandrát and M.V. Lokajiček, *Phys. Rev. D* **31**, 1045 (1985); *Phys. Lett B* **232**, 263 (1989); *Z. Phys. C* **63**, 619 (1994); *Phys. Rev. D* **55** (1997) (to be published).
- [28] M. Kawasaki, T. Maehara, and M. Yonezawa, *Phys. Rev. D* **55** (1997) (to be published).
- [29] A.F. Martini and M.J. Menon, in *1994 XV Brazilian National Meeting on Particles and Fields*, Angra dos Reis, RJ, 1994 (Sociedade Brasileira de Física, São Paulo, 1995) p. 208.
- [30] J.B. Bronzan, G.L. Kane and U.P. Sukhatme, *Phys. Lett.* **B49**, 227 (1974).
- [31] Differential cross section data at $\sqrt{s} = 13.8$ and 19.4 GeV: D.S. Ayres *et al.*, *Phys. Rev. D* **15**, 3105 (1977); C.W. Akerlof *et al.*, *Phys. Rev. D* **14**, 2864 (1976); G. Fidecaro *et al.*, *Phys. Lett.* **B105**, 309 (1981); R. Rubinstein *et al.*, *Phys. Rev. D* **30**, 1413 (1984).
- [32] ρ data at $\sqrt{s} = 13.8$ and 19.4 GeV: L.A. Fajardo *et al.*, *Phys. Rev. D* **24**, 46 (1981).
- [33] C. Augier *et al.*, *Phys. Lett.* **B316**, 448 (1993).
- [34] E. Gotsman, E.M. Levin, and U. Maor, *Z. Phys. C* **57**, 677 (1993).
- [35] H. Cheng and T.T. Wu, *Expanding protons: scattering at high energies* (MIT Press, Cambridge, MA, 1987).
- [36] P.R. Bevington and D.K. Robinson, *Data reduction and error analysis for the physical sciences*, (McGraw-Hill , New York, 1992).
- [37] A.F. Martini and M.J. Menon, in *1995 XVI Brazilian National Meeting on Particles and Fields*, Caxambu, MG, 1995 (Sociedade Brasileira de Física, São Paulo, 1996) p. 305.
- [38] A.S. Carrol *et al.*, *Phys. Lett.* **B61**, 303 (1976); A.S. Carrol *et al.*, *Phys. Lett.* **B80**, 423 (1979).
- [39] P. Giromini *et al.* (CDF Collaboration), in *Proceedings of the Fifth International Conference on Elastic and Diffractive Scattering*, edited by H.M. Fried, K. Kang, and C.-I. Tan (World Scientific, Singapore, 1994), p. 30.
- [40] L.Lukaszuk and B. Nicolescu, *Nuovo Cimento Lett.* **8**, 405 (1973); P. Gauron, E. Leader and B. Nicolescu, *Phys. Rev. Lett.* **B54**, 2656 (1985); **B55**, 639 (1985).
- [41] M. Giffon, E. Predazzi, and A. Samokhin, *Phys. Lett.* **B375**, 315 (1996).
- [42] T.T. Chou and C.N. Yang, in *High Energy Physics and Nuclear Structure*, edited by G. Alexander (North-Holland, Amsterdam, 1967), p. 348; *Phys. Rev.* **170**, 1591 (1968); *Phys. Rev. Lett.* **20**, 1213 (1968).
- [43] R. Henzi and P. Valin, *Phys. Lett B* **132**, 443 (1983); *Phys. Lett B* **160**, 167 (1985).
- [44] U. Amaldi, M. Jacob, and G. Matthiae, *Ann. Rev. Nucl. Sci.* **26**, 385 (1976).
- [45] R.J. Glauber and J. Velasco, *Phys. Lett. B* **147**, 380 (1984); in *Proceedings of the Second International Conference on Elastic and Diffractive Scattering*, edited by K. Goulianos (Editions Frontières, Gif-Sur-Yvette, 1988), p. 219.
- [46] M. Kamran and I.E. Qureshi, in *Proceedings of the Second International Conference on Elastic and Diffractive Scattering*, edited by K. Goulianos (Editions Frontières, Gif-Sur-Yvette, 1988), p. 289; *Hadronic J.* **12**, 25 (1989); **12**, 173 (1989).
- [47] M. Saleem, F. Aleem, and I.A. Azhar, *Europhys. Lett.* **6**, 201 (1988); F. Aleem, M. Saleem and G.B. Yodh, *J. Phys. G* **16**, L269 (1990).

FIG. 1. Results for the elastic pp differential cross section at $\sqrt{s} = 52.8$ GeV. The imaginary part of the amplitude was calculated using previous parametrizations [17,18] and the real part through (a) Martin prescription (8), and (b) the ansatz (10), with $\lambda = 0.055$. In both cases it is shown the contributions from the real part (dotted), imaginary part (dashed) and complex amplitude (solid). Experimental data on $d\sigma/dt$ are from [3] and the ρ value in Martin's formula from [2].

FIG. 2. Values of the free parameters C and α^{-2} , from Table I, that fit experimental data (circles) and parametrizations through (16) and (17) (solid line).

FIG. 3. Values of the free parameter λ , from Table I, that fit experimental data (circles) and parametrizations through (18) in the cases (19) (dot) and (20) (dash).

FIG. 4. Model predictions for the differential cross sections in cases 1, Eq. (19), and 2, Eq. (20) (indistinguishable) and experimental data ([31] for $\sqrt{s} = 13.8$ and 19.4 GeV and [3] for the other energies). Curves and data were multiplied by factors of $10^{\pm 2}$.

FIG. 5. Model predictions for the ρ parameter (left) and total cross section (right) in cases 1, Eq. (19) (solid), and 2, Eq. (20) (dash) and experimental data ([2] and [32] for ρ and [2] and [38] for the total cross section).

FIG. 6. Predictions for the ρ parameter in cases 1 and 2 and experimental data (Fig. 5).

FIG. 7. Predictions for the proton-proton total cross section and experimental informations: accelerator data [2,38] (crosses), Akeno [4] (circles), Nikolaev [6] (triangles), GSY limit at 30 TeV [5] (\uparrow) and GSY result at 40 TeV [5] (square).

FIG. 8. Predictions for the pp differential cross section at 10 (solid), 15 (dash) and 20 TeV (dot).

FIG. 9. Radius calculated through Eq. (21) with $\beta^2 = 1.80 \text{ GeV}^2$ and parametrization (17) for α^{-2} .

FIG. 10. Inelastic Overlap Function calculated from the eikonal through Eqs. (22) and (23).

FIG. 11. Predictions for the dimensionless quantity $C\alpha^2$ (see text) and points from fit (Table I).

TABLE I. Values of the free parameters from fits of pp differential cross section and ρ data at each energy.

\sqrt{s} (GeV)	C(s) (GeV ⁻²)	α^{-2} (s) (GeV ⁻²)	λ (s)	$C\alpha^2$
13.8	9.970	2.092	-0.094	4.77
19.4	10.050	2.128	0.024	4.72
23.5	10.250	2.174	0.025	4.71
30.7	10.370	2.222	0.053	4.67
44.7	10.890	2.299	0.079	4.74
52.8	11.150	2.370	0.099	4.70
62.5	11.500	2.439	0.121	4.72

Fig. 1 authors A.F. Martini and M.J. Menon

title Multiple diffraction model for proton-proton elastic ...

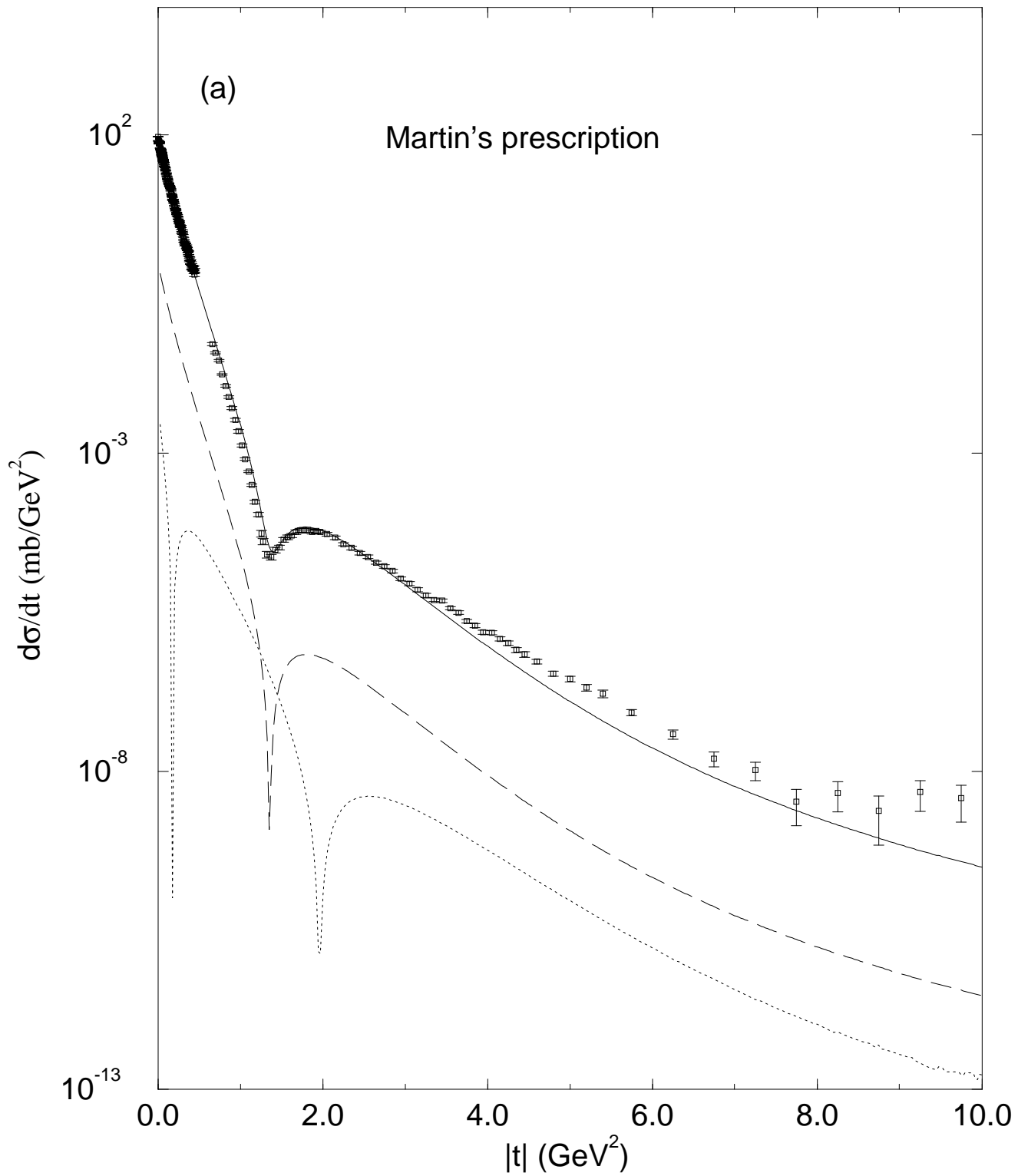


Fig.1 authors A.F. Martini and M.J. Menon

title Multiple diffraction model for proton-proton elastic ...

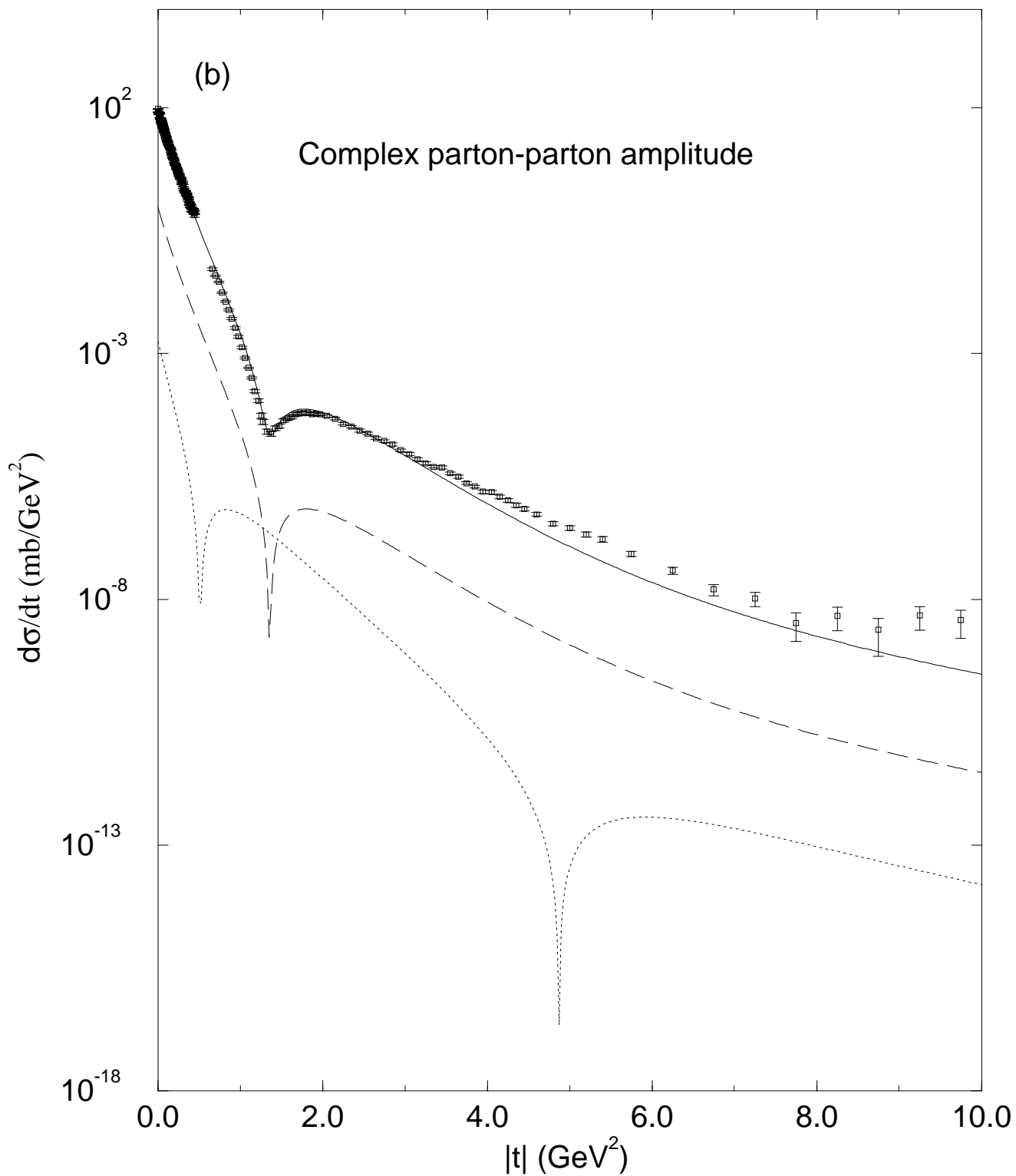


Fig. 2 authors A.F. Martini and M.J. Menon

title Multiple diffraction model for proton-proton elastic ...

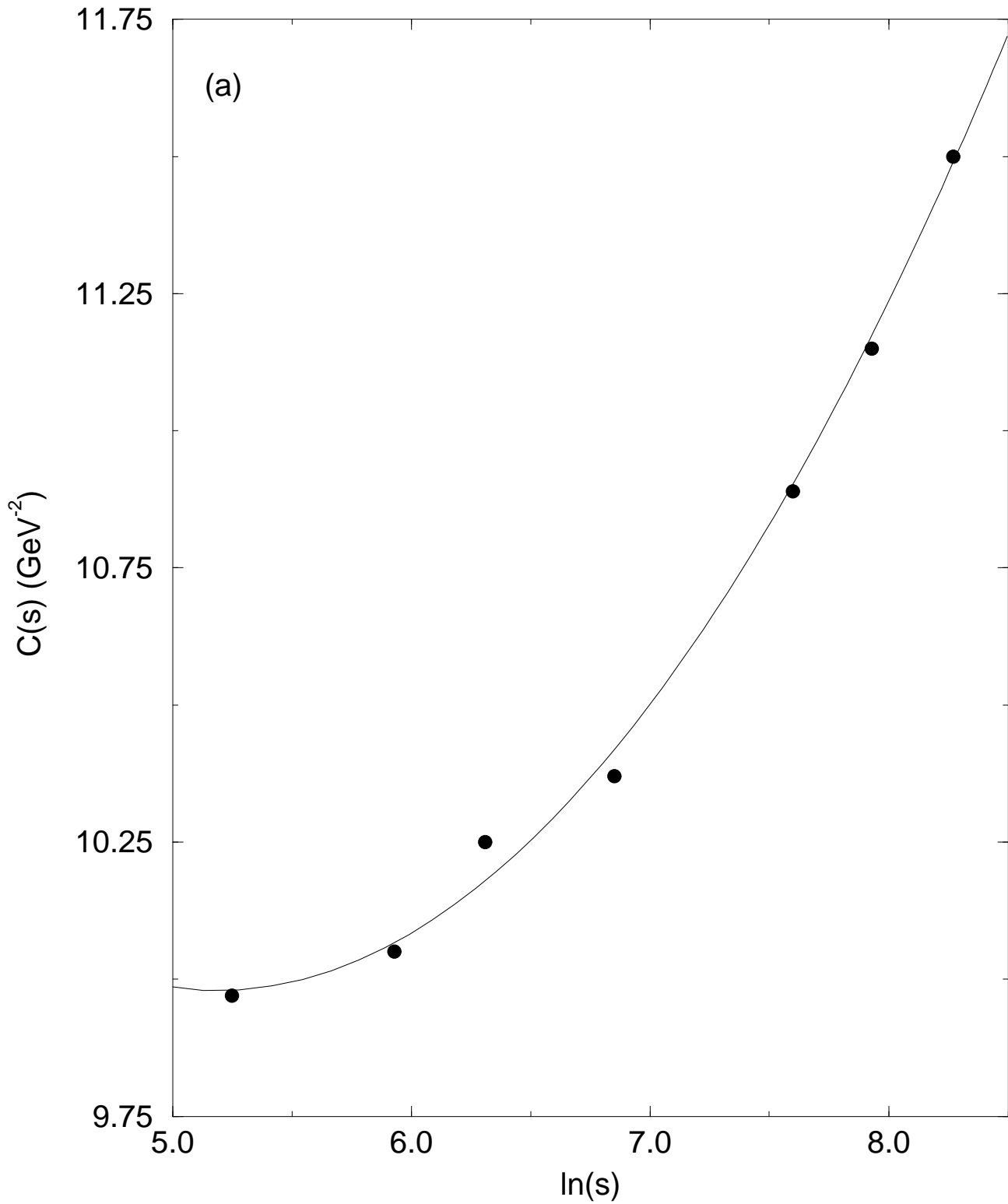


Fig. 2 authors A.F. Martini and M.J. Menon

title Multiple diffraction model for proton-proton elastic ...

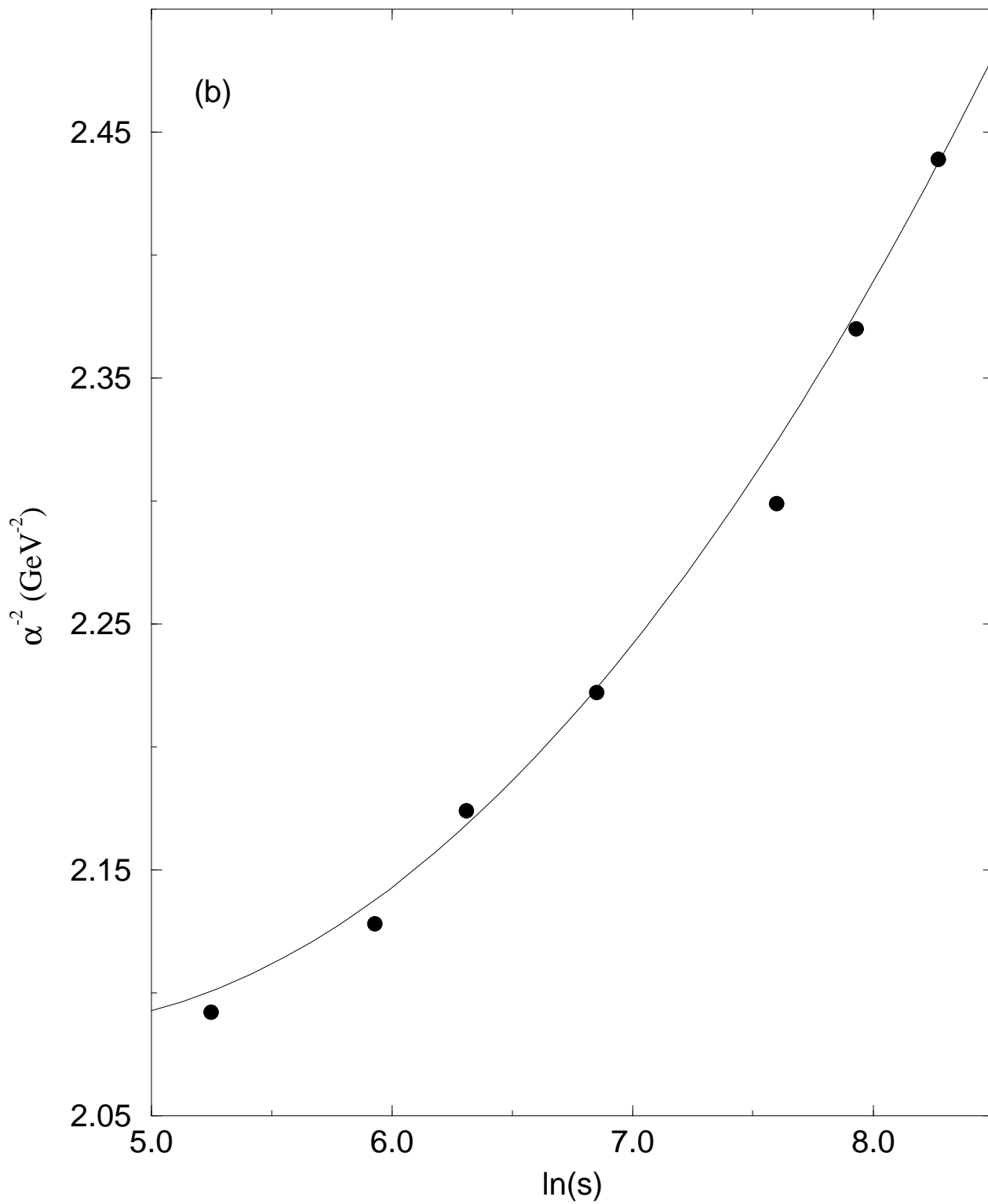


Fig. 3 authors A.F. Martini and M.J. Menon

title Multiple diffraction model for proton-proton elastic ...

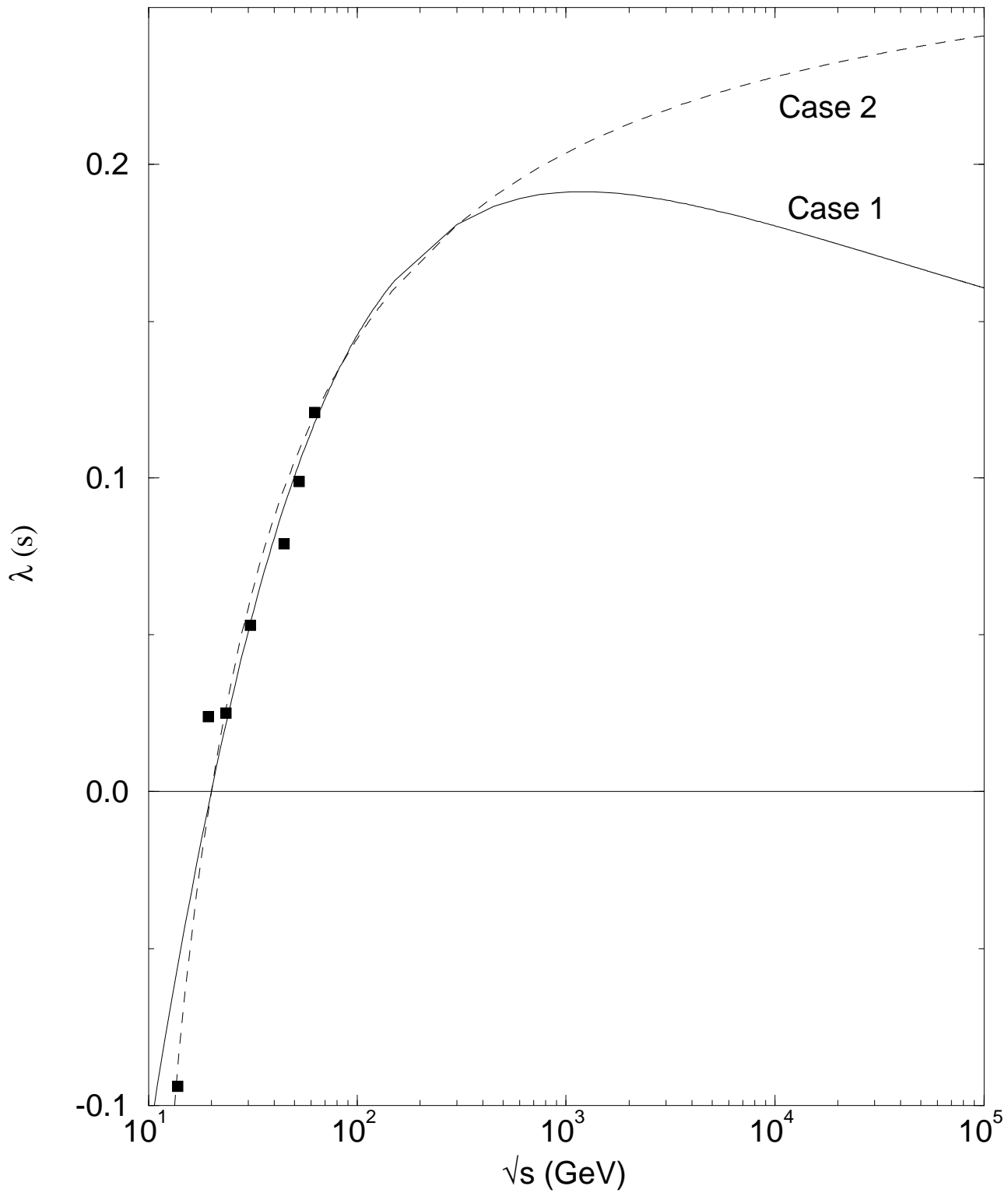


Fig. 4 authors A.F. Martini and M.J. Menon

title Multiple diffraction model for proton-proton elastic ...

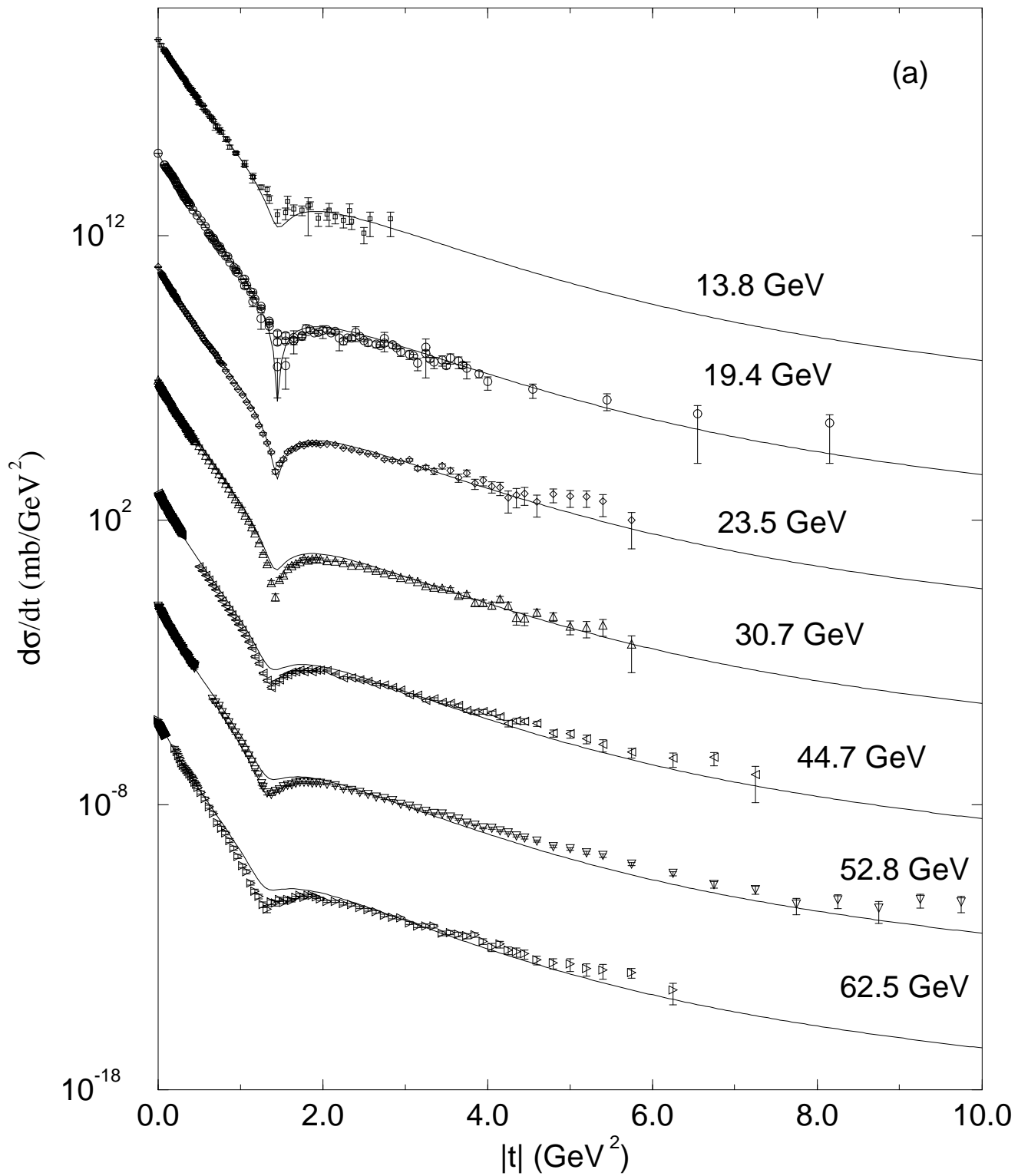


Fig. 4 authors A.F. Martini and M.J. Menon
title Multiple diffraction model for proton-proton elastic ...

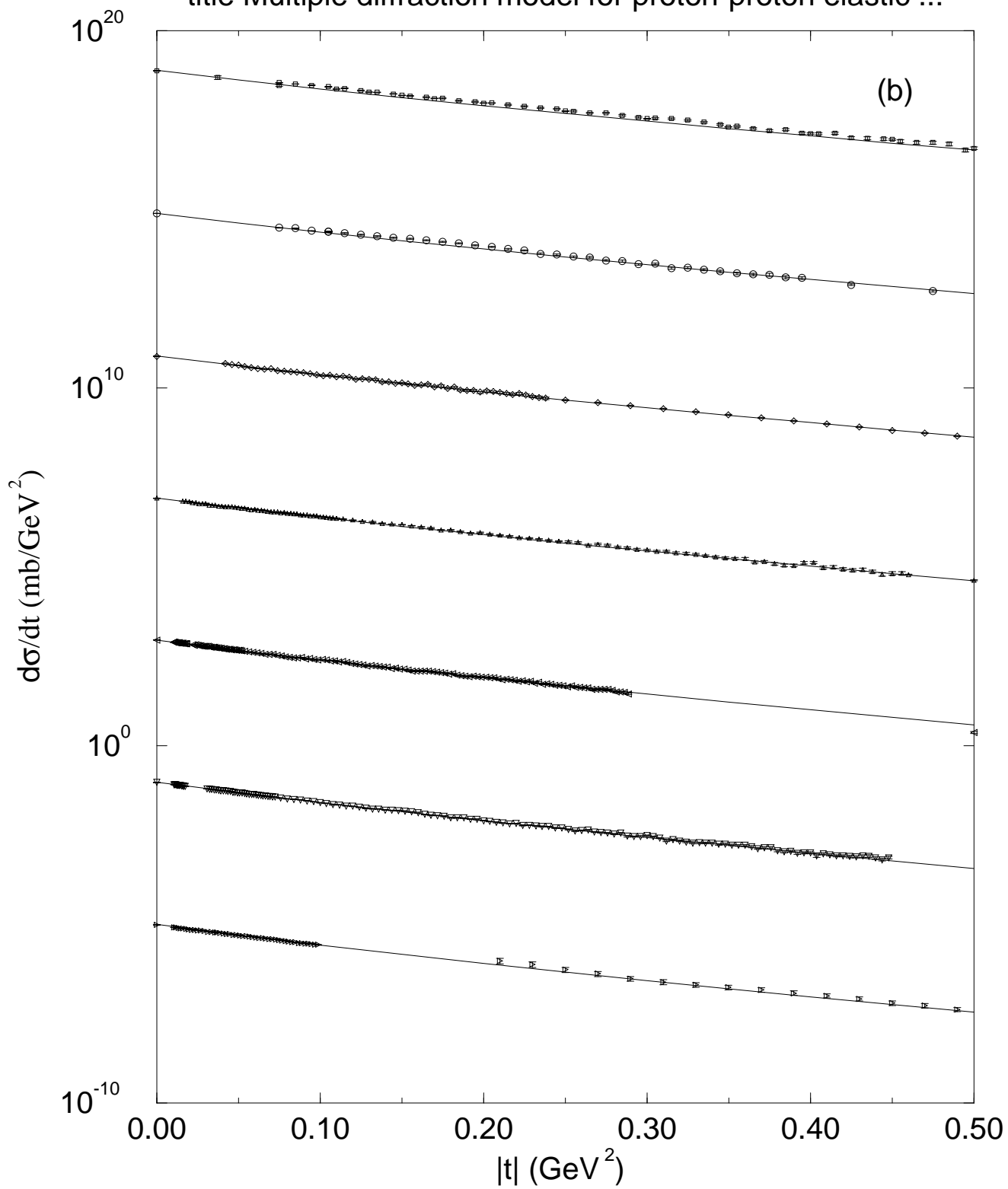


Fig. 5 authors A.F. Martini and M.J. Menon

title Multiple diffraction model for proton-proton elastic ...

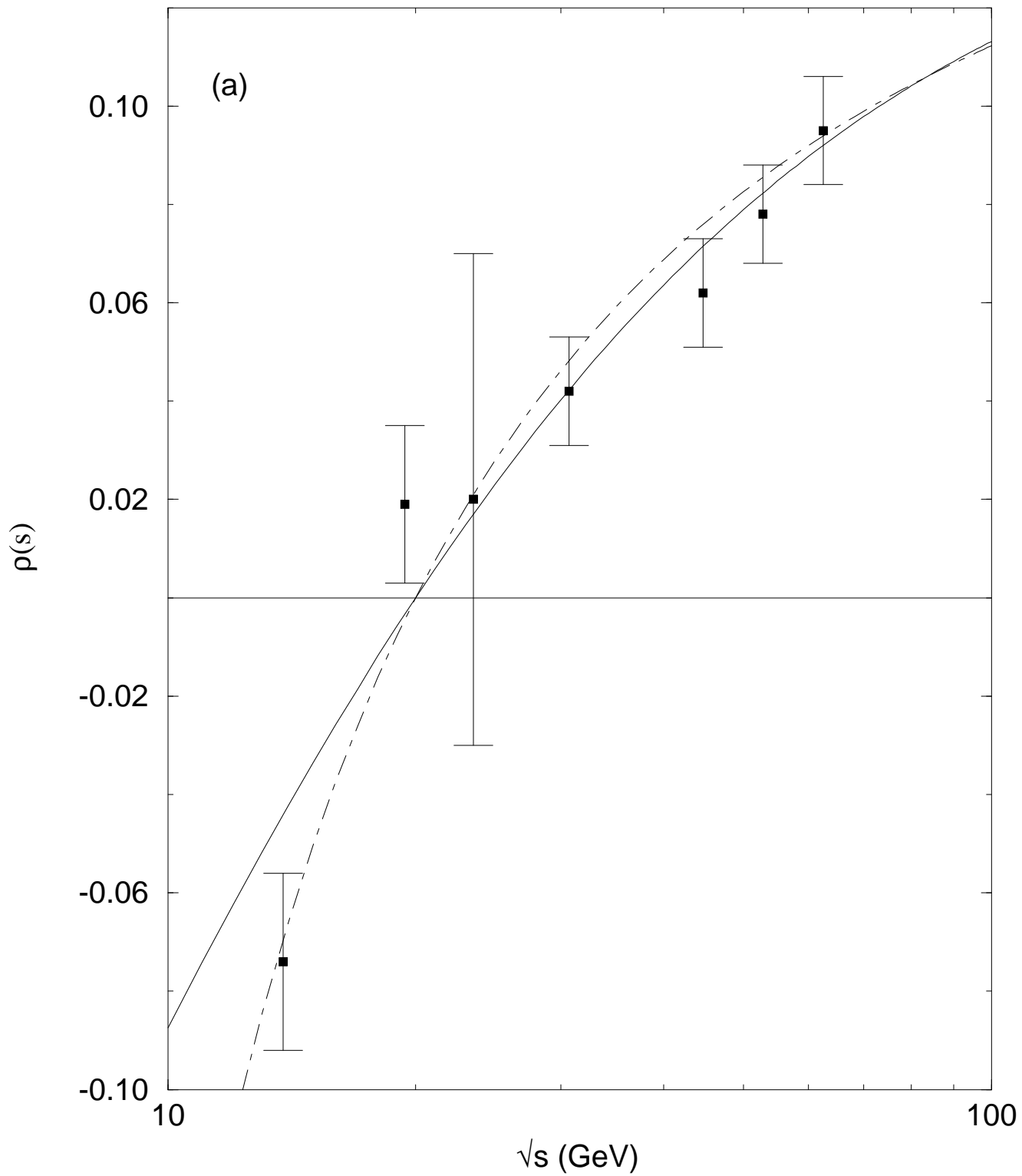


Fig. 5 authors A.F. Martini and M.J. Menon

title Multiple diffraction model for proton-proton elastic ...

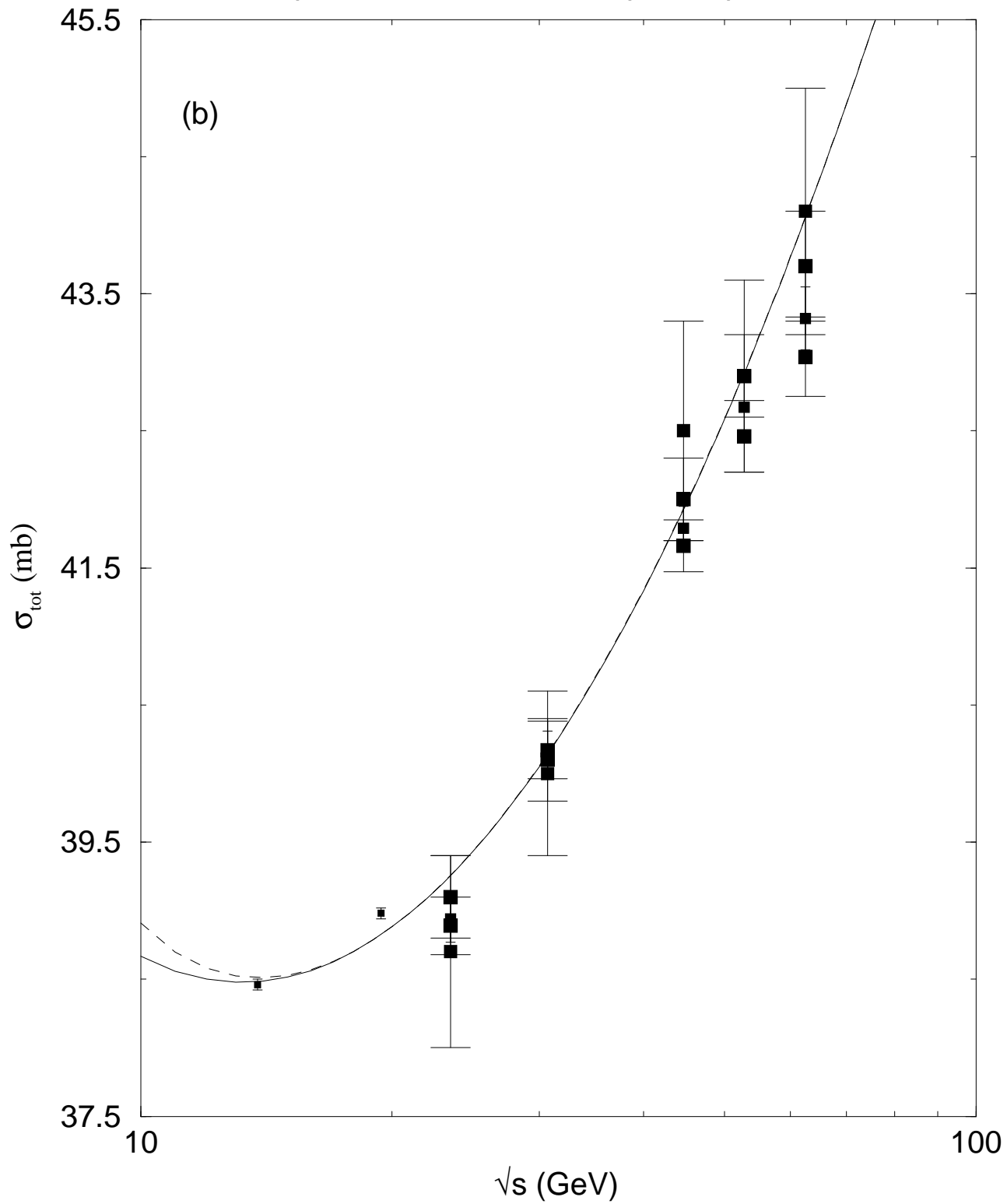


Fig. 6 authors A.F. Martini and M.J. Menon

title Multiple diffraction model for proton-proton elastic ...

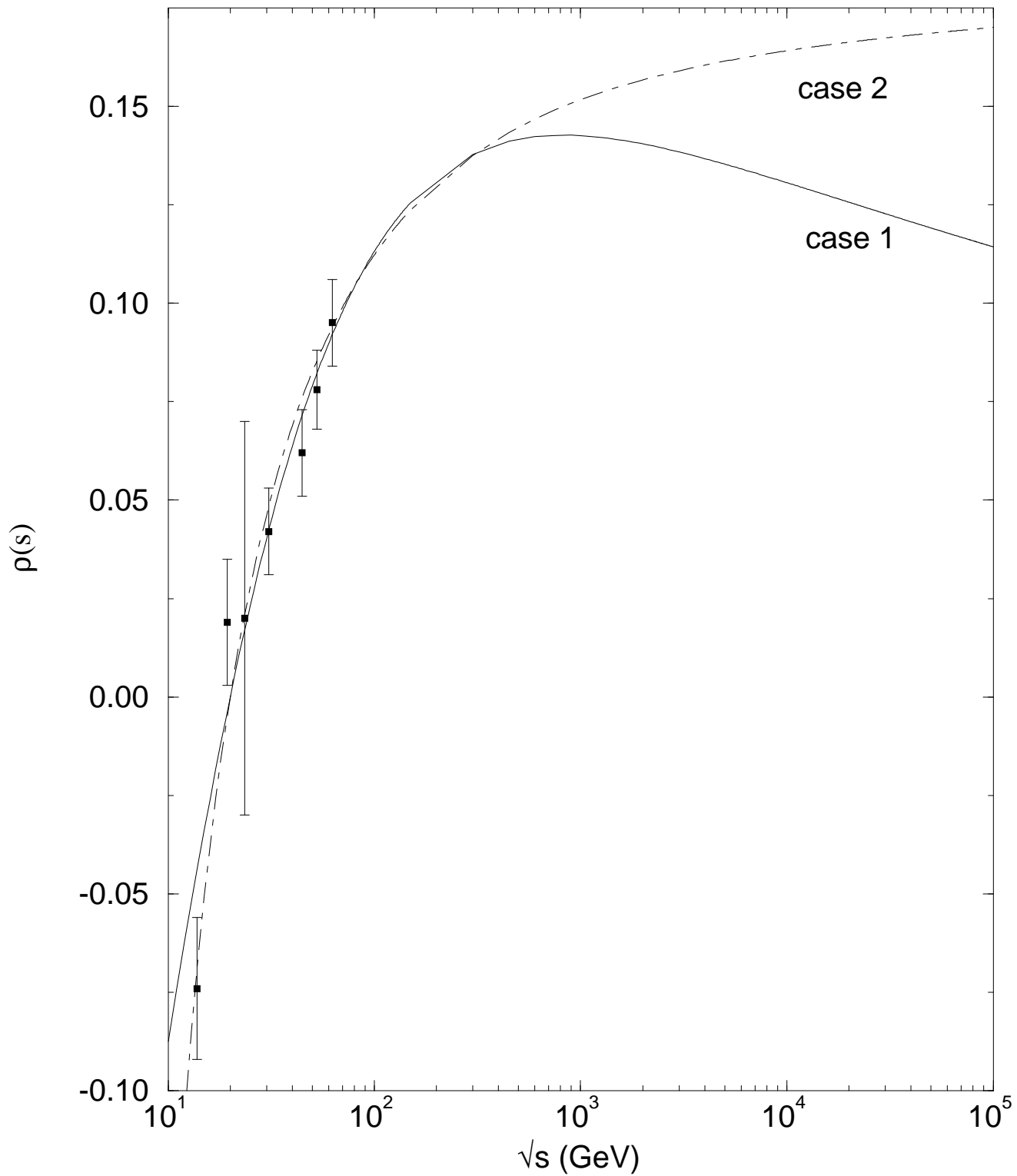


Fig. 7 authors A.F. Martini and M.J. Menon

title Multiple diffraction model for proton-proton elastic ...

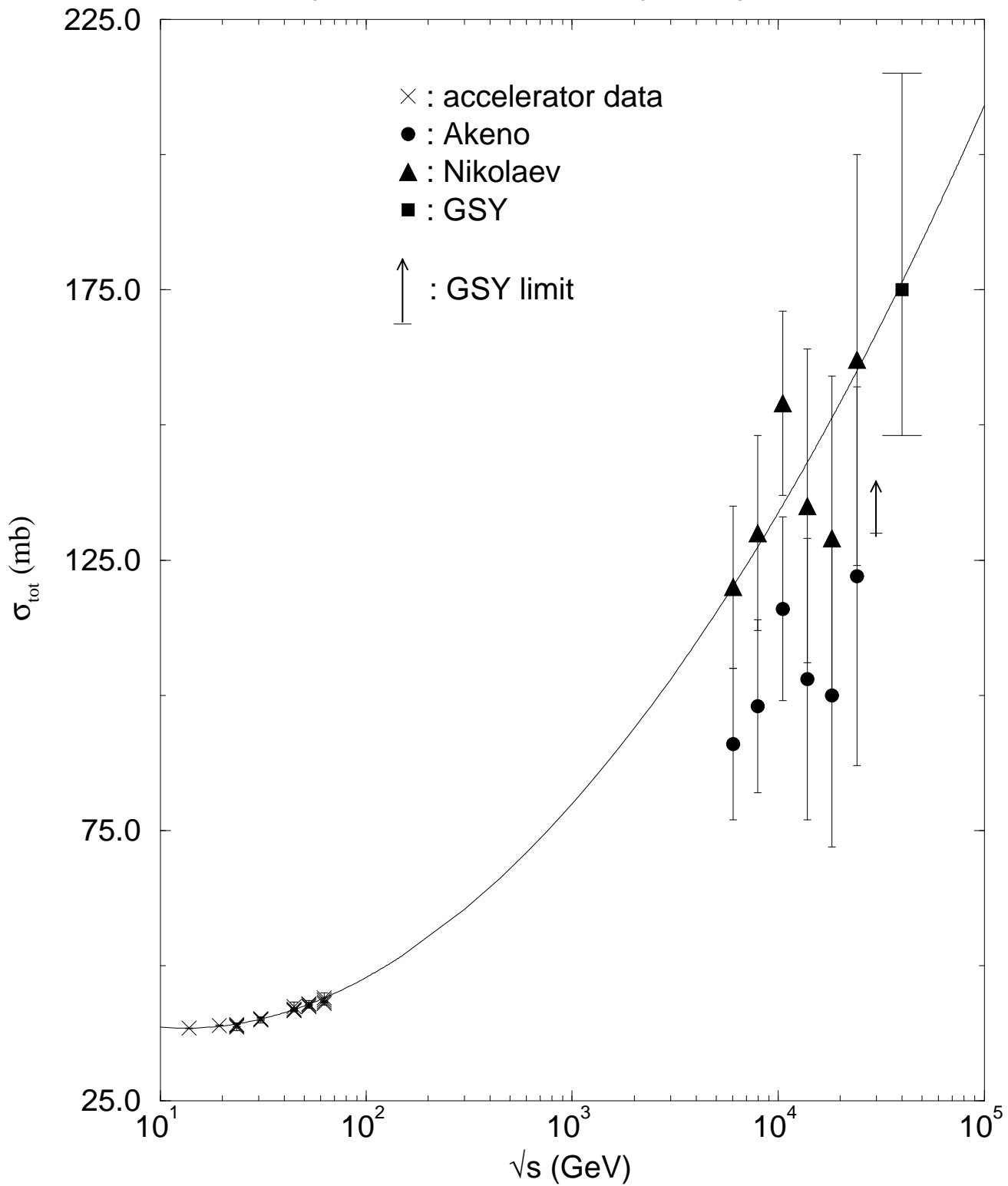


Fig. 8 authors A.F. Martini and M.J. Menon

title Multiple diffraction model for proton-proton elastic ...

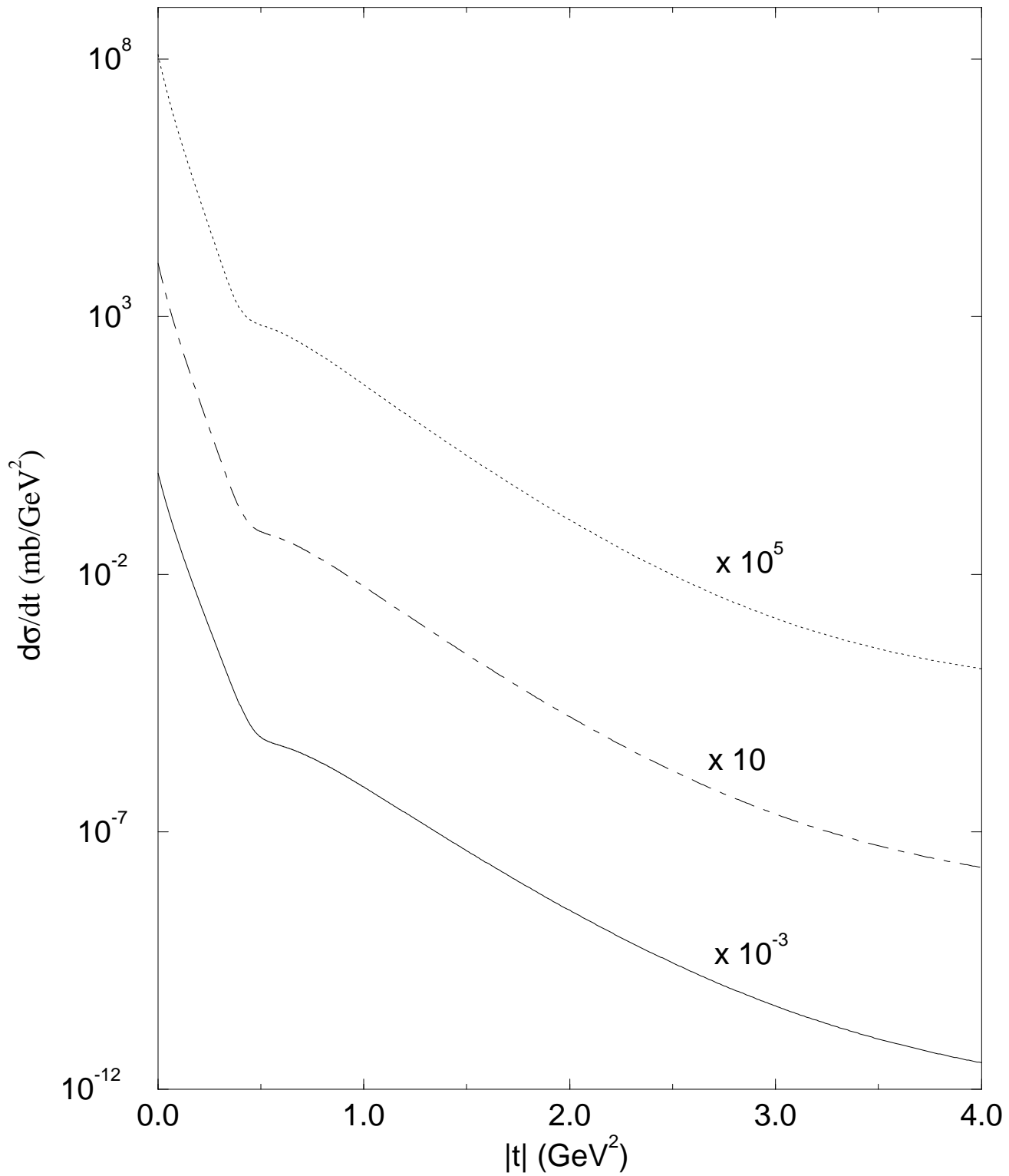


Fig. 9 authors A.F. Martini and M.J. Menon

title Multiple diffraction model for proton-proton elastic ...

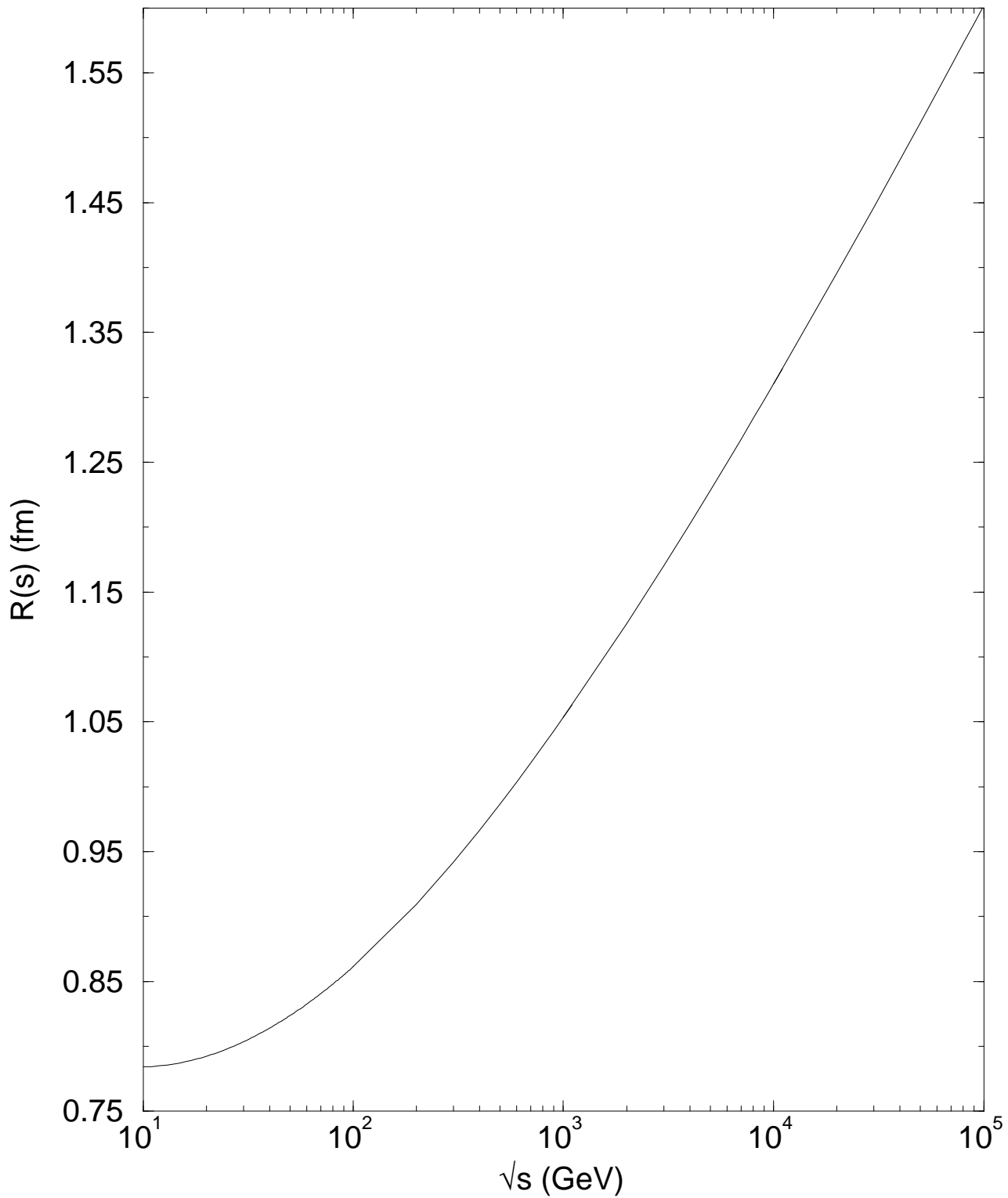


Fig. 10 authors A.F. Martini and M.J. Menon

title Multiple diffraction model for proton-proton elastic ...

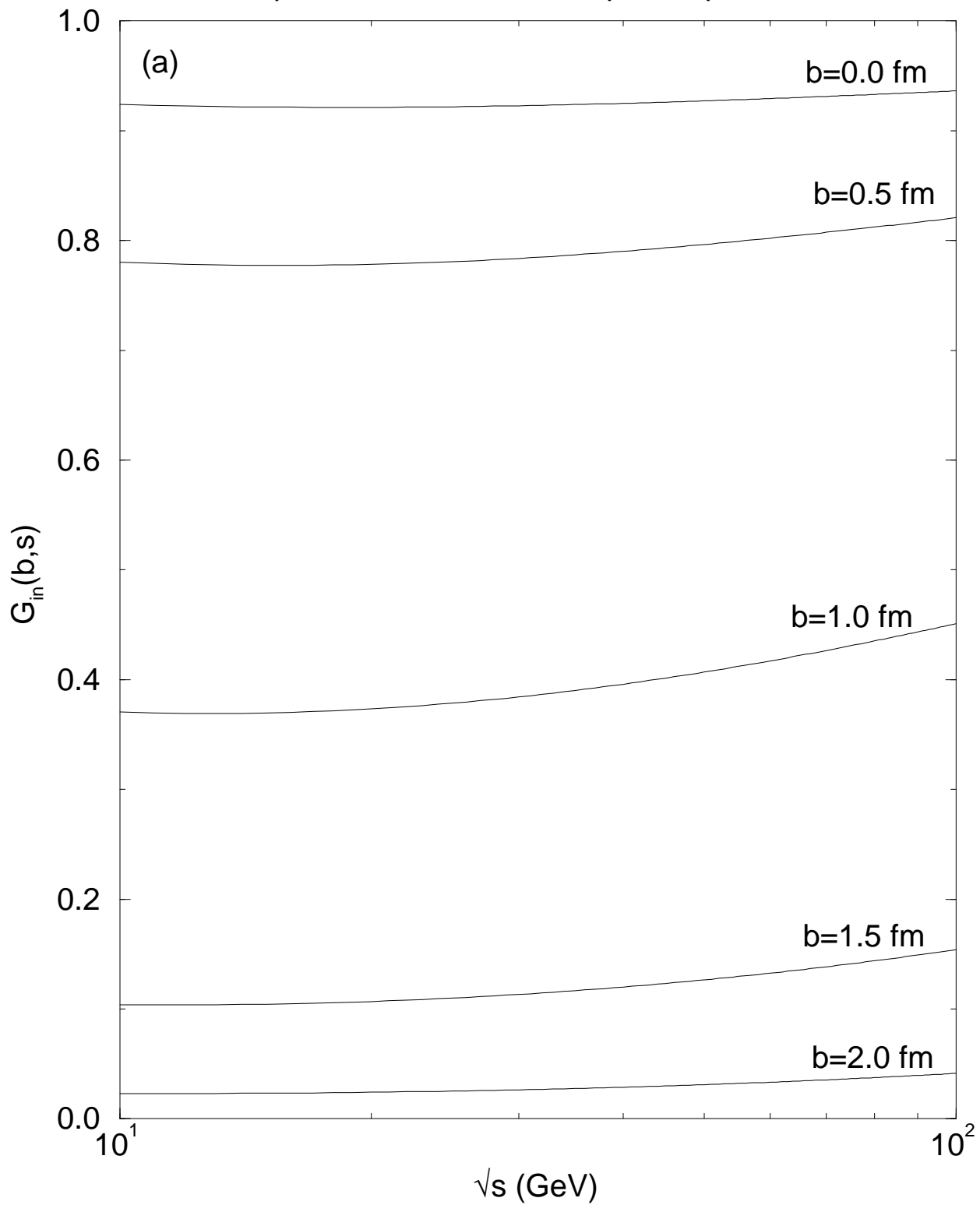


Fig. 10 authors A.F. Martini and M.J. Menon

title Multiple diffraction model for proton-proton elastic ...

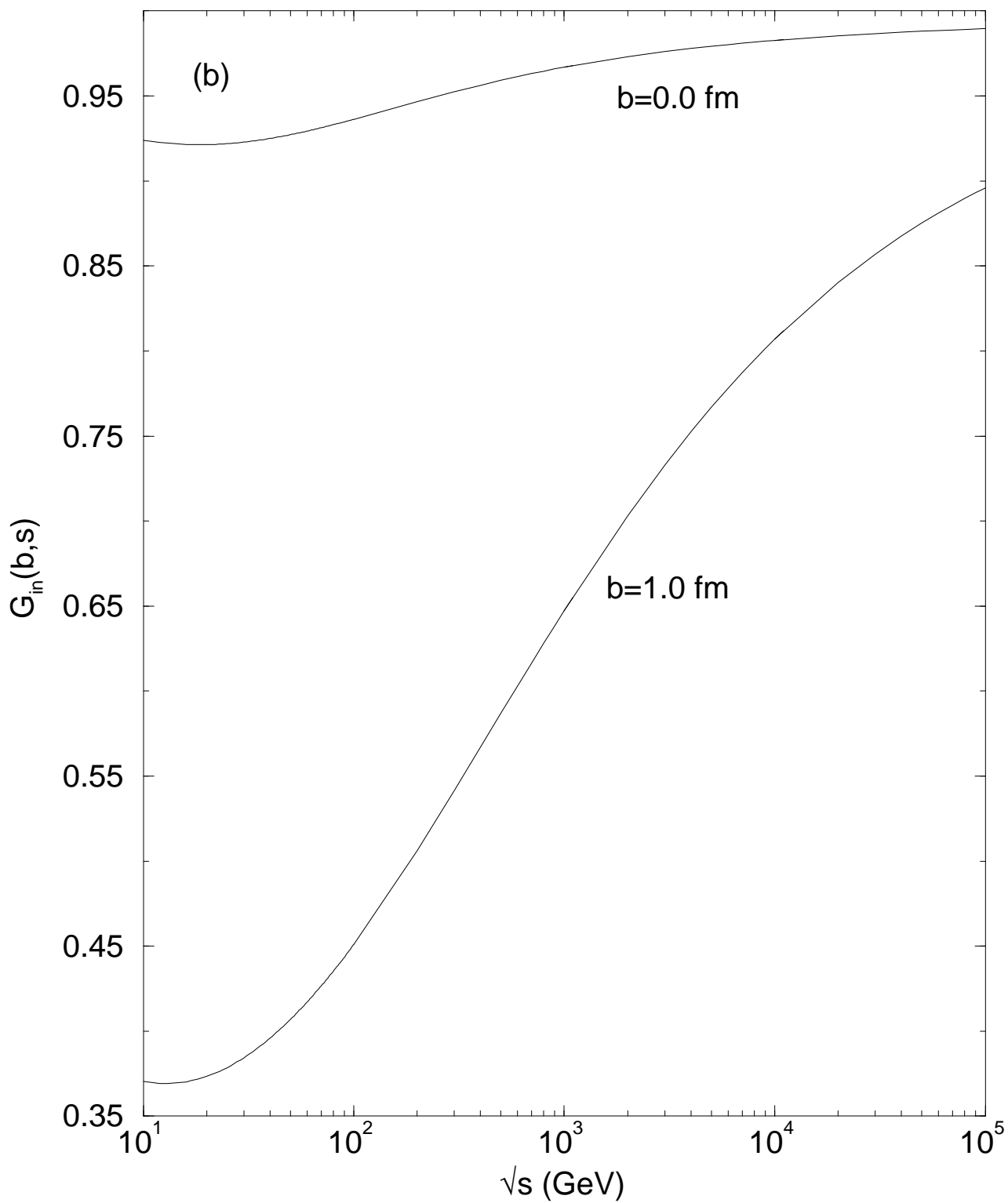


Fig. 11 authors A.F. Martini and M.J. Menon

title Multiple diffraction model for proton-proton elastic ...

